Optical Properties of $As_{36}Te_{42}Ge_{10}Si_{12}$ Thin Films

N.A. Hegab[a], H.M. El-Mallah[b]

[a]Faculty of Education, Ain Shams University, Roxy — Cairo, Egypt

[b]Dept of Physics & Mathematical Engineering, Faculty of Engineering, Port-Said University, 42524 Port-Said, Egypt

(Received October 22, 2009; in final form March 22, 2010)

Thermally evaporated $As_{36}Te_{42}Ge_{10}Si_{12}$ amorphous chalcogenide films were prepared in a vacuum of 10^{-5} Torr on to glass substrates hold at about 300 K during the deposition process. Measurements of the optical properties have been made. The optical transmittance and reflectance spectra of films in the thickness range 155–395 nm were measured in the wavelength λ range 500–2500 nm. The refractive index n, the extinction coefficient k and the absorption coefficient α were calculated for the studied films. It is found that both n and k are independent on the film thickness. The refractive index n has anomalous behavior for the wavelength λ range 500–1500 nm, while it has normal dispersion for the wavelength greater than 1500 nm. The optical energy gap was estimated from absorption coefficient. The allowed optical transitions were found to be nondirect transitions with optical gap of 1.08 eV for the sample under test. The effect of annealing on the obtained optical parameters was also investigated.

PACS numbers: 78.20.–e, 78.20.Ci, 78.66.–w, 78.68.+m

1. Introduction

Amorphous semiconductor films have been investigated from the point of view of basic physics as well as of device technology for various applications. Chalcogenide glasses represent one of the major categories of amorphous semiconductors. In the recent years, considerable attention has been focused on these materials (glasses), due to their threshold and memory switching effects and the infrared transmission of many of these glasses which make them potential materials of industrial applications in memory devices, fiber optics, guided wave devices and infrared telecommunication systems [1–10]. When these glasses are irradiated with high energy particles or light, bond breaking and bond rearrangement can take place, which result in the change in local structure of the glassy materials, which leads to changes in the optical constants [11, 12] and absorption edge shift [13], which make these materials suitable for the fabrication of the large number of optical devices. Thus, the estimation of the optical parameters of chalcogenide glasses is obviously necessary in order to know the basic mechanism underlying these phenomena, and also to exploit and develop their technological applications.

Optical properties are important in view of the extensive interest in the optoelectronic devices. The optical properties were studied for $As_{36}Te_{42}Ge_{10}Si_{12}$ films deposited on glass substrates with different thickness 155–395 nm, using optical reflectance R and transmittance T data for the spectral region 500–2500 nm. The reflectance and transmittance data were analyzed to determine the optical constants: refractive index n, extinction coefficient k and absorption coefficient α. Analysis of the refractive index n results have been carried out to obtain the high frequency dielectric constant ε_∞ and other related parameters. Analysis of the absorption coefficient α has been carried out to estimate the optical band gap and determine the nature of transitions involved.

2. Experimental

Bulk $As_{36}Te_{42}Ge_{10}Si_{12}$ glass was prepared under vacuum of 10^{-5} Torr by quenching from the melt as mentioned before [9]. Thin films were prepared by thermal evaporation technique on well cleaned glass substrates of suitable dimensions. The cleaned substrates were placed adjacent to a selected holder. A cleaned silica boat was charged with small granules of the prepared material and placed in the electrical spiral heater of the coating unit. The glass substrates were placed at a tangent to a suitable holder temperature, and the vacuum chamber was pumped down to 10^{-5} Torr. Then the boat temperature was gradually raised in steps according to a certain regime given before [9]. Samples with different thicknesses were prepared under the same evaporation conditions. The substrate temperature was held below 50 ℃ during deposition. The film thickness was established by Tolansky's method [14] using multiple beam Fizeau fringes. The film thickness was ranged from 155 to 395 nm.

The optical distribution of the reflectance R and transmittance T of the samples were measured at room temperature by normal incidence of light in the wavelength λ range from 500 to 2500 nm in steps of 2 nm using a double beam spectrophotometer (Jasco 570). These data are analyzed to determine the optical constants: the refractive index n, the extinction coefficient k and the absorption coefficient α. An analysis of the absorption coefficient has also been carried out in order to estimate the optical

band-gap and the nature of the involved optical transitions. Also the effect of annealing on the optical constants and optical energy gap was investigated. Films were annealed in air at 373, 423 and 463 K for one hour.

The amorphicity was carefully checked for all investigated films by the absence of any diffraction lines in their X-ray patterns [9]. On annealing at 463 K films have a polycrystalline structure [7].

3. Results and discussion

The study of the optical properties of the investigated sample particularly the absorption edge has proved to be a very useful to explore the electronic structure of thin film sample. In the following section we study the transmittance T and reflectance R for the studied films. The spectral distribution of the refractive index n, the extinction coefficient k and the absorption coefficient α were determined. The analysis of the absorption coefficient α has been carried out to obtain the optical energy gap $E_{\mathrm{g}}^{\mathrm{opt}}$ and the Urbach tail of localized states E_{e}. The analysis of the refractive index n with the help of the extinction coefficient k has been carried out to obtain the real part of the complex dielectric constant ε'.

3.1. Determination of optical constants

Figures 1a and b show the spectral distribution curves of reflectance R and the transmittance T for the composition $As_{36}Te_{42}Ge_{10}Si_{12}$ films of the thickness 155–395 nm at room temperature. The data from these curves have been used to compute the refractive index n and the extinction coefficient k, using the Murmann's exact equations [15].

For normal incidence the amplitude of Fresnel's coefficients of reflection in the case of the absorbing thin film deposited on glass substrate is given by the following relations:

The refractance $R_{(n,k)}$ is given by:

$$R_{(n,k)} = \frac{Ae^{\beta} + Be^{-\beta} + 2C\cos\alpha + 4D\sin\alpha}{Ee^{\beta} + Fe^{-\beta} + 2G\cos\alpha + 4H\sin\alpha}\,. \tag{1}$$

The transmittance, $T_{(n,k)}$, can be easily derived to give the following form:

$$T_{(n,k)} = \frac{16n_{\mathrm{o}}n_{\mathrm{q}}(n^2+k^2)}{Ee^{\beta} + Fe^{-\beta} + 2G\cos\alpha + 4H\sin\alpha}\,, \tag{2}$$

where

$$\begin{aligned}
A &= [(n-n_{\mathrm{o}})+k^2][(n-n_{\mathrm{q}})+k^2]\,,\\
B &= [(n-n_{\mathrm{q}})+k^2][(n-n_{\mathrm{o}})+k^2]\,,\\
C &= (n^2+k^2)(n_{\mathrm{o}}^2+n_{\mathrm{q}}^2) - (n^2+k^2)^2 - n_{\mathrm{o}}^2n_{\mathrm{q}}^2\\
&\quad -4n_{\mathrm{o}}n_{\mathrm{q}}k^2\,,\\
D &= k(n_{\mathrm{q}}-n_{\mathrm{o}})(n^2+k^2+n_{\mathrm{o}}n_{\mathrm{q}})\,,\\
E &= [(n-n_{\mathrm{o}})^2+k^2][(n+n_{\mathrm{q}})^2+k^2]\,,\\
F &= [(n-n_{\mathrm{o}})^2+k^2][(n-n_{\mathrm{q}})^2+k^2]\,,\\
G &= (n^2+k^2)(n_{\mathrm{o}}^2+n_{\mathrm{q}}^2) - (n^2+k^2)^2 - n_{\mathrm{o}}^2n_{\mathrm{q}}^2\\
&\quad +4n_{\mathrm{o}}n_{\mathrm{q}}k^2\,,\\
H &= k(n_{\mathrm{q}}-n_{\mathrm{o}})(n^2+k^2-n_{\mathrm{o}}n_{\mathrm{q}})\,,
\end{aligned}$$

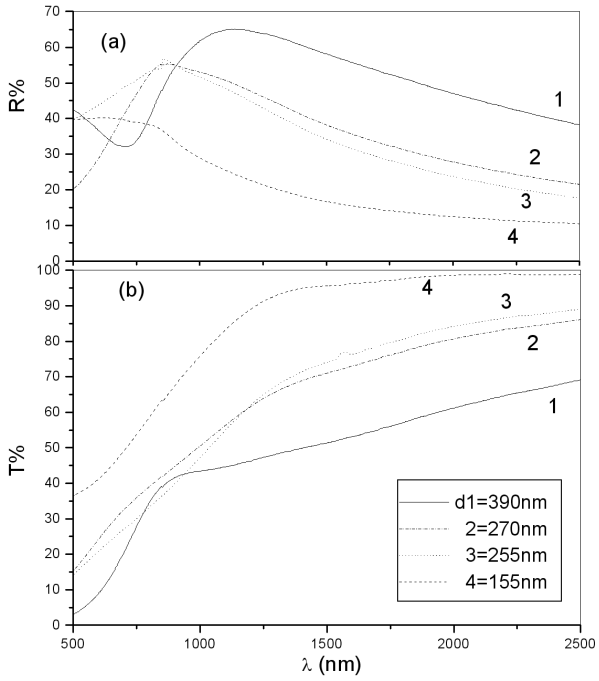

Fig. 1. (a) Spectral behavior of reflectance R for $As_{36}Te_{42}Ge_{10}Si_{12}$ films of different thicknesses: (b) spectral behavior of transmittance T for $As_{36}Te_{42}Ge_{10}Si_{12}$ films of different thicknesses.

$$\begin{aligned}
&n_{\mathrm{o}} = 1.0 \quad \text{for air}\,,\\
&n_{\mathrm{q}} = 1.52 \quad \text{for glass}\,,\\
&\alpha = \frac{4\pi t}{\lambda}n\,, \quad \text{and} \quad \beta = \frac{4\pi t}{\lambda}k\,.
\end{aligned}$$

A computer program comprising a modified search technique is used. It is based on minimizing $(\Delta T)^2$ and $(\Delta R)^2$ simultaneously presented, where

$$(\Delta T)^2 = |T_{(n,k)} - T_{\mathrm{exp}}|^2, \tag{3}$$

$$(\Delta R)^2 = |R_{(n,k)} - R_{\mathrm{exp}}|^2, \tag{4}$$

T_{exp} and R_{exp} are the experimentally determined absolute values of T and R, respectively, and $T_{(n,k)}$ and $R_{(n,k)}$ are the values of T and R calculated by using the Murmann's exact equations [15].

Figures 2a and b show the spectral distribution of both n and k for the studied films. The discrepancies in the obtained results lie within the acceptable range of experimental error ($\pm 4\%$ for n and ± 2.5 for k). Accordingly both n and k are independent on the film thickness in the investigated range. It is observed that the refractive index n shows anomalous dispersion in the wavelength range 500–1500 nm, while it has normal dispersion for the wavelength greater than 1500 nm. Also it is clearly evident from these figures that the values of n and k decrease with increasing the wavelength through the investigated range.

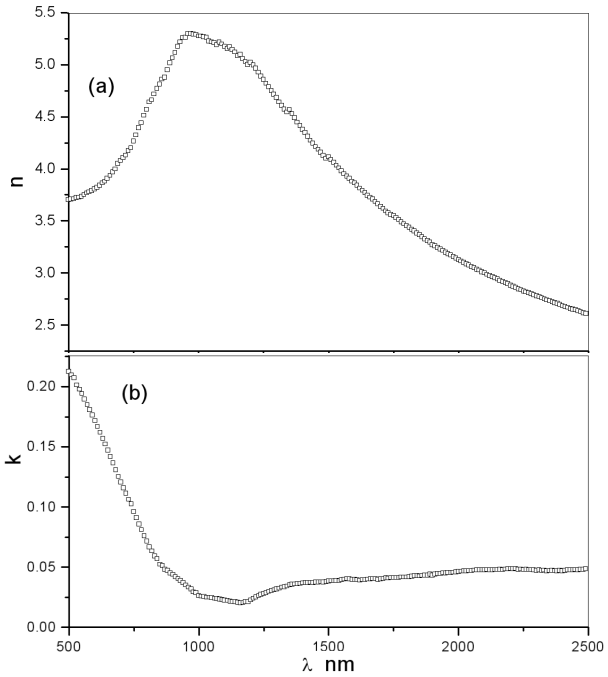

Fig. 2. (a) Spectral distribution of the refractive index n as a function of wavelength λ for $As_{36}Te_{42}Ge_{10}Si_{12}$ films; (b) spectral distribution of the extinction coefficient k as a function of wavelength λ for $As_{36}Te_{42}Ge_{10}Si_{12}$ films.

3.2. Analysis of refractive index

The obtained data of refractive index can be analyzed to obtain the high frequency dielectric constant ε_∞ via the following procedure. This procedure describes the contribution of the free carriers and the lattice vibration modes of the dispersion. The real part of dielectric constant ε' and the square of wavelength λ^2 is related by the following relation [16]:

$$\varepsilon' = n^2 - k^2 = \varepsilon_\infty - B\lambda^2, \tag{5}$$

where

$$B = e^2 N/4\pi^2 c^2 \varepsilon_o m^*, \tag{6}$$

n is the refractive index, k is the extinction coefficient, ε_∞ is the lattice dielectric constant or the high frequency dielectric constant, λ the wavelength, e the electron charge, N the free charge carrier concentration, ε_o the permittivity of the free space, m^* is the effective mass of the charge carrier and c is the velocity of light.

Figure 3 shows the relation between ε' versus λ^2 plots for the studied films. From this figure, one can see ε' decreases at longer wavelengths. To obtain the high frequency dielectric constant ε_∞, Eq. (5) was applied to the linear part of the relation between ε' and λ^2. The intersection at $\lambda^2 = 0$ for the linear part of this curve at high wavelength gave the value of ε_∞ and the slope of this part give the ratio N/m^*. The estimated values of ε_∞ and the ratio N/m^* are presented in the Table.

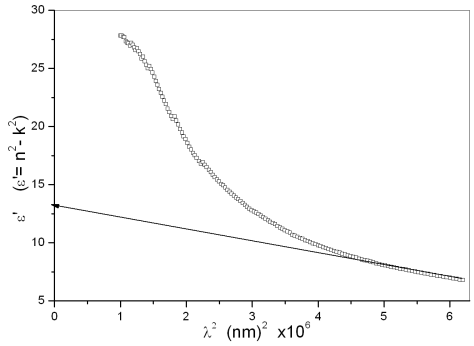

Fig. 3. The dependence of ε' on λ^2 for $As_{36}Te_{42}Ge_{10}Si_{12}$ of as-deposited films.

TABLE

Values of the optical parameters for as-deposited and annealed $As_{36}Te_{42}Ge_{10}Si_{12}$ films.

Sample [K]	E_g [eV]	E_e [eV]	α_o [cm^{-1}]	ε_∞	N/m^* [cm^{-3} kg^{-1}] × 10^{45}
As-deposited	1.08	0.124	6.54	13.28	2.00
373	0.96	0.135	1.85	14.50	2.55
423	0.77	0.143	17.26	27.93	5.42
463	0.75	0.163	52.24	85.42	17.03

3.3. Analysis of extinction coefficient

The spectral distribution of the absorption coefficient α was calculated for the studied films at different values of the wavelength λ in the considered spectrum region using the corresponding values of k and the well known relation $\alpha = 4\pi k/\lambda$. The spectral distribution of the optical absorption coefficient α can be divided into two regions:

(i) In the first region, the absorption coefficient $\alpha < 10^4$ cm^{-1}, there is usually an Urbach tail [17] where $\alpha(\nu)$ depends exponentially on the photon energy $h\nu$ according to the following relation:

$$\alpha(\nu) = \alpha_o \exp(h\nu/E_e)\,, \tag{7}$$

where ν is the frequency of the radiation, α_o is a constant, h is the Planck's constant and E_e is often interpreted as the width of the tails of localized states in the gap region, and in general it represents the degree of disorder in amorphous semiconductor [18]. Therefore by plotting the relation $\ln\alpha = f(h\nu)$ as shown in Fig. 4, both values of α_o and E_e for the studied films can be estimated and given in the Table.

(ii) For higher values of the absorption coefficient α $(\nu) \geq 10^4$ cm^{-1}, this corresponds to transition between states in both valence and conduction bands, where the absorption coefficient α for the studied films can be described by the following relation [19, 20]:

$$\alpha h\nu = A(h\nu - E_g^{opt})^r, \tag{8}$$

where A is a constant, E_g^{opt} is the optical energy gap of the material and r is the power which characterizes the

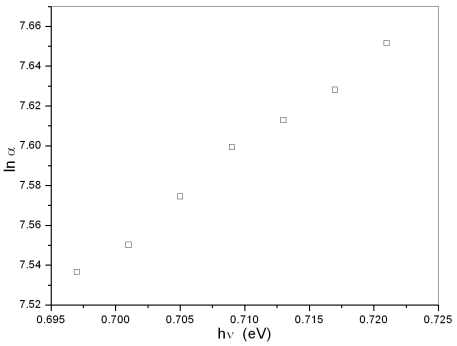

Fig. 4. Plot of $\ln(\alpha)$ *vs.* $(h\nu)$ for $As_{36}Te_{42}Ge_{10}Si_{12}$ of as-deposited films.

transition process. r has value $1/2$ for the direct allowed transition and the value 2 for the indirect allowed transition (nondirect in case of amorphous semiconductor). The functional dependence of the optical absorption coefficient $(\alpha h\nu)^{1/2}$ versus the photon energy $h\nu$ is shown in Fig. 5 for the studied films. It is clear from this figure that the plot of $(\alpha h\nu)^{1/2} = f(h\nu)$ is a linear function, and this linearity indicates the existence of the allowed indirect (nondirect in case of an amorphous semiconductors) transition. The intercept of the extrapolation of the linear part to zero absorption with photon energy axis is taken as the value of the forbidden energy gap E_g^{opt} is independent of film thickness and equal to 1.08 eV.

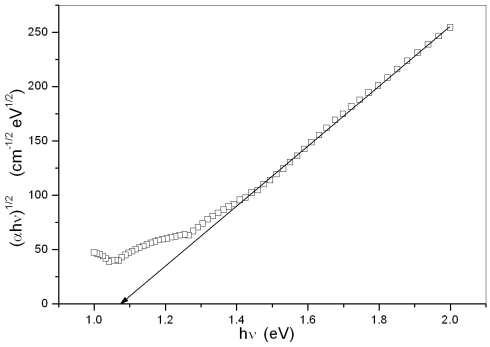

Fig. 5. Dependence of $(\alpha h\nu)^{1/2}$ on the photon energy $h\nu$ for $As_{36}Te_{42}Ge_{10}Si_{12}$ of as-deposited films.

3.4. Effect of annealing

To investigate the dependence of the optical properties of $As_{36}Te_{42}Ge_{10}Si_{12}$ films, samples of different thicknesses in the range mentioned above were annealed for one hour at 373, 423 and 463 K. The reflectance R and transmittance T were measured for annealed films over the spectral range mentioned above. The spectral dependence of the refractive index n for the annealed films and the extinction coefficient k for $As_{36}Te_{42}Ge_{10}Si_{12}$ annealed films are shown in Figs. 6a and b. The value of refractive index n increases while the value of extinction coefficient k decreases with increasing of the wavelength λ. Values of n increases also for annealed films as it is shown in Fig. 6a, in comparison with the as-deposited films for all wavelengths range. It is observed also that the peak which shown in refractive index n shifts to lower energies for annealing films. This shift is associated with the decrease in the optical energy gap E_g^{opt}.

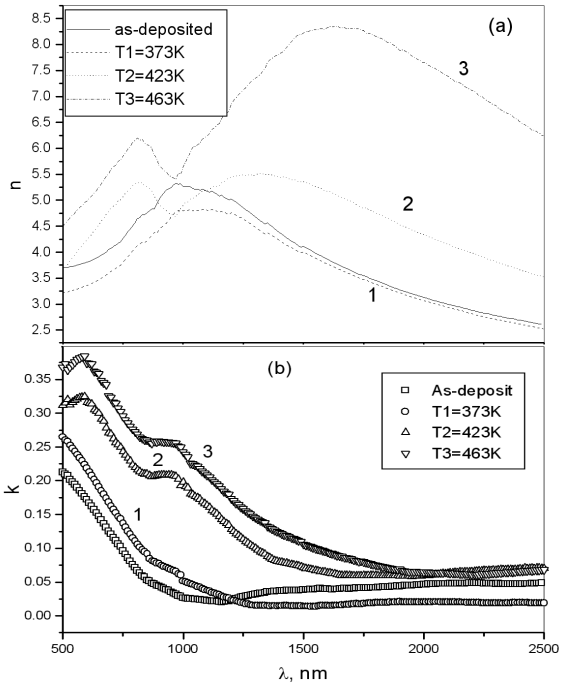

Fig. 6. (a) Spectral distribution of the refractive index n as a function of wavelength λ for $As_{36}Te_{42}Ge_{10}Si_{12}$ of as-deposited and annealed films; (b) spectral distribution of the extinction coefficient k as a function of wavelength λ for $As_{36}Te_{42}Ge_{10}Si_{12}$ of as-deposited and annealed films.

The obtained results of the refractive index n were analyzed to obtain the high frequency dielectric constant ε_∞ following the same procedure mentioned above. The values of ε_∞ and N/m^* were also given in Table for the annealed films. By using the same procedure, the extinction index k and absorption coefficient α were determined. Figure 7a represents the spectral behavior of the absorption coefficient α as a function of photon energy $h\nu$ for the deposited and annealed films.

For the absorption coefficient $\alpha < 10^4$ cm^{-1}, the width of Urbach's tail E_e can be calculated for the studied films annealing at different temperatures as mentioned above using the data in Fig. 7b and Eq. (7). The variation of $(\alpha h\nu)^{1/2}$ with photon energy $h\nu$ is shown in Fig. 8. It is clear from this figure that the optical absorption mechanism is still due to nondirect transitions according to Eq. (8), and the absorption edge was shifted towards the lower photon energy side. From plots of a least square fit, the values of energy gap E_g^{opt} for annealed films was determined from Fig. 8. It is observed from this figure that E_g^{opt} decreased with annealing temperatures 373,

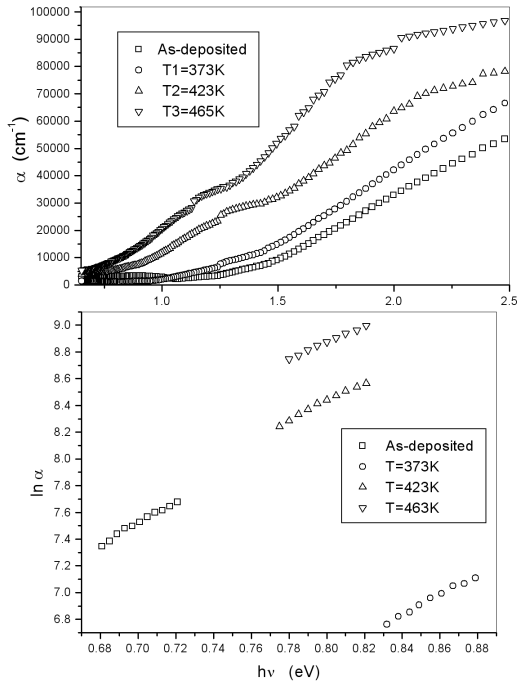

Fig. 7. (a) Spectral behavior of absorption coefficient, α, for $As_{36}Te_{42}Ge_{10}Si_{12}$ of as-deposited and annealed films; (b) plots of $\ln(\alpha)$ vs $(h\nu)$ for $As_{36}Te_{42}Ge_{10}Si_{12}$ of as-deposited and annealed films.

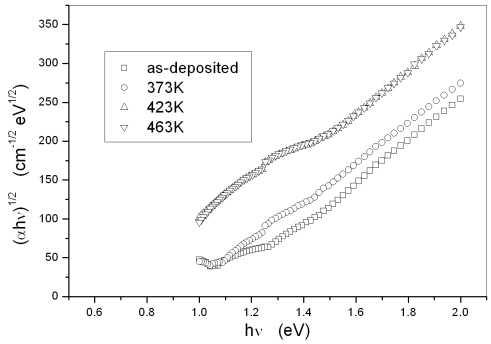

Fig. 8. Dependence of $(\alpha h\nu)^{1/2}$ on the photon energy $(h\nu)$ for $As_{36}Te_{42}Ge_{10}Si_{12}$ of as-deposited and annealed films.

423 and 463 K. The obtained values of E_g^{opt}, E_e and α_o are given in Table. From this table, it is clear that the energy gap decreases, the absorption coefficient increases, and the width of the Urbach tail increases with thermal annealing. Since E_e is generally considered to represent the degree of disorder [15], an increase in the annealing temperature leads to increase in the width of localized states, *i.e.* the disorder within the films increases.

Amorphous thin films usually contain unsaturated bonds which result of an insufficient number of atoms deposited in the films. These bonds are responsible for the formation of some defects in the films. Such defects produce localized states in the band gap of amorphous materials. When the amorphous films are annealed in low temperature the optical energy gap increases. The observed changes in the optical energy gap have been analyzed on the basis of the theory proposed by Mott and Davis [21] for amorphous materials. During annealing, the unsaturated defects are gradually annealed out [22] producing large numbers of saturated bonds. The reduction in the number of unsaturated defects decreases the density of localized states in the band structure and consequently increases the optical energy gap and decrease in the width of the band tail. When the films are annealed at higher temperatures values, there is enough energy is present to break some weaker bonds [20] and resulting in an increase in the number of unsaturated bonds which are responsible for the formation of some types of defects in the structure of the studied films. As the number of these defects increases with increase of annealing temperature, the concentration of localized states in the band structure also increases gradually. Hence the annealing process of the films causes an increase of the energy width of localized states thereby reducing the optical energy gap [23–25]. This conclusion can explain the observed decrease of the optical energy gap of the studied films annealed at higher temperature values.

4. Conclusions

The study of the optical properties of $As_{36}Te_{42}Ge_{10}Si_{12}$ thin films indicate that the absorption mechanism is due to an indirect transitions in the studied thickness range 155–395 nm and wavelength range 500–2500 nm. Both n and k for the as-deposited films are practically independent of the film thickness. Analysis of the refractive index n yield high frequency dielectric constant ε_∞ and the ratio of the free charge carrier concentration to the effective mass of the charge carrier N/m^*. Annealing $As_{36}Te_{42}Ge_{10}Si_{12}$ films shows a decrease of the optical energy gap E_g^{opt} with increasing of the annealing temperatures. The refractive index n, the extinction coefficient k and the high frequency dielectric constant ε_∞ increase with increasing annealing temperatures of the studied film composition.

References

[1] A.V. Stronski, in: *Proc. NATO Advanced Research Workshop on Micro-Electronic Interconnections and Assembly*, Eds. G. Harman, P. Mach, Kluwer Academic, Netherlands 1998.

[2] K. Tanaka, *Phys. Rev. B* **39**, 1270 (1989).

[3] P. Nermec, M. Frumar, B. Frumarova, M. Jelinek, J. Lancok, J. Jedelsky, *Opt. Mat.* **15**, 191 (2000).

[4] P. Nermec, M. Frumar, J. Jedelsky, M. Jelinek, J. Lancok, I. Gregora, *J. Non-Cryst. Solids* **299-302**, 1013 (2002).

[5] S.R. Ovshinsky, in: *Disorder Materials Science and Technology*, Ed. D. Adler, Amorphous Institute Press, New York 1982.

[6] S.R. Ovshinsky, *Phys. Rev. Lett.* **21**, 1450 (1968).

[7] M.A. Afifi, N.A. Hegab, *Vacuum* **49**, 135 (1997).

[8] N.A. Hegab, M. Fadel, M.M. El-Samanody, *J. Mat. Sci.* **30**, 5461 (1995).

[9] N.A. Hegab, *J. Phys. D, Appl. Phys.* **33**, 2353 (2000).

[10] R.M. Mehra, R. Kumar, P.C. Mathur, *Thin Solid Films* **170**, 15 (1989).

[11] L. Tichy, H. Ticha, P. Nagels, R. Callaerts, R. Mertens, M. Vlcek, *Mat. Lett.* **39**, 122 (1999).

[12] J.M. Gonzalez-Leal, A. Ledesma, A.M. Bermal-Oliva, R. Prieto-Alcon, E. Marquez, J.A. Angel, J. Carabe, *Mat. Lett.* **39**, 232 (1999).

[13] V.M. Lyubin, M. Klebanov, B. Sfez, B. Ashkinadze, *Mat. Lett.* **58**, 1706 (2004).

[14] S. Tolansky, *Multiple-beam Interferometery of surfaces and films*, Oxford University Press, London 1948, p. 147.

[15] M. Murmann, *Z. Phys.* **80**, 161 (1933); *Z. Phys.* **101**, 643 (1936).

[16] J.N. Zemel, J.D. Jensen, R.B. Schoolar, *Phys. Rev. A* **140**, 330 (1965).

[17] J. Tauc, in: *Amorphous and liquid semiconductors*, Ed. J. Tauc, Plenum, New York 1974, p. 159.

[18] J. Olley, *Solid State Commun.* **13**, 1437 (1973).

[19] J. Bardeen, F.J. Blatt, L.H. Hall, In.R. Breckenridge, B. Russel, T. Hahn, in: *Proc. Photo Conductivity Conf.*, Wiley, New York 1956.

[20] E.A. Davis, N.F. Mott, *Philos. Mag.* **22**, 903 (1970).

[21] N.F. Mott, E.A. Davis, *Electronic Process in non--crystalline Matrials*, Clarendon Press, Oxford 1979.

[22] S. Hasegawa, S. Yazalci, T. Shimizu, *Solid State Commun.* **26**, 407 (1978).

[23] N.A. Afifi, *J. Non-Cryst. Solids* **128**, 279 (1991).

[24] A.A. Abu-Sehly, M.I. Abd-Elrahman, *J. Phys. Chem. Sol.* **36**, 136 (2001).

[25] S. Chaudhuri, S.K. Biswas, *J. Non-Cryst. Solids* **54**, 179 (1983).